Journal of Photochemistry and Photobiology A: Chemistry 220 (2011) 145–152

Contents lists available at ScienceDirect

Journal of Photochemistry and Photobiology A: Chemistry

journal homepage: www.elsevier.com/locate/jphotochem

Interaction of a ruthenium(II)–chalcone complex with double stranded DNA: Spectroscopic, molecular docking and nuclease properties

Ruchi Gaur[a], Rais Ahmad Khan[b], Sartaj Tabassum[b], Priyanka Shah[c], Mohammad I. Siddiqi[c], Lallan Mishra[a,*]

[a] Department of Chemistry, Faculty of Science, Banaras Hindu University, Varanasi-221005, India
[b] Department of Chemistry, Aligarh Muslim University, Aligarh 202002, India
[c] Molecular and Structural Biology Division, Central Drug Research Institute, Lucknow-226001, India

ARTICLE INFO

Article history:
Received 30 December 2010
Received in revised form 23 March 2011
Accepted 2 April 2011
Available online 14 April 2011

Keywords:
Ru(II) complex
X-ray crystallography
DNA binding
Molecular docking
Gel electrophoresis

ABSTRACT

The interaction of a well characterized new complex **1** *cis,fac*-[RuCl(dmso-S)$_3$(L)] LH = 1-(2-hydroxyphenyl)-3-(4-chlorophenyl) propenone with Calf-thymus DNA (CT-DNA) is monitored using UV–vis titration ($K_b = 3.8 \times 10^7$) and ethidium bromide displacement studies ($K_{sv} = 3.2$). The molecular docking of the complex with DNA sequence d(ACCGACGTCGGT)$_2$ reveals that complex is stabilized by additional electrostatic and hydrogen bonding interaction with DNA besides probable displacement of a labile DMSO by the N^7 of guanine. The coordination of guanine is further supported by the isolation and characterization of its adduct with the complex 1.gua (gua = guanine). The nuclease property of complex **1** in the absence and presence of different activators and trappers demonstrates that complex efficiently cleaves supercoiled pBR322 plasmid DNA and binds through major groove of the DNA.

1. Introduction

The interaction of transition metal complexes with DNA is found interesting owing to their probable applications in cancer therapy, molecular biology [1,2] and photodynamic therapy (PDT) [3]. In this context, after cisplatin and carboplatin, ruthenium complexes are explored extensively for their antitumor properties [4]. A preliminary understanding of such properties has been explored by targeting DNA molecule [5]. The ruthenium metal ions appended with ligand like dimethyl sulphoxide has been exploited due to labile nature of dmso molecule providing its easy substitution with biomolecules. Thus, such ligand frame work is considered as important building block in the construction of metal based active drug [6]. The Ru(II) centre bearing labile ligands could form monofunctional adducts with DNA. However, among complexes containing π-bonded ligands, metal arenes form hydrophobic and van der Waals contacts with nucleobases [7]. Thus, a combination of suitable metal as well as design of ligand is considered important prerequisite for the construction of a highly efficient drug. Chalcones, being an important class of ligands due to their novel structure as well diverse bioactivities [8,9] like anticancer, anti-inflammatory, antimalarial, antifungal and antiviral agents are considered important components in the construction of overall geometry of the metal complexes. The chalcones are also exploited as a precursor for the synthesis of flavones, potential antioxidant. Thus, a chalcone is considered 'privileged structure' [10]. Based on these precedence, initially a well known ruthenium(II) complex *cis,fac*-[RuCl$_2$(dmso-*S*)$_3$(dmso-*O*)] was allowed to react with 1-(2-hydroxyphenyl)-3-(4-chlorophenyl)-propenone(LH). The resulting composition *cis,fac*-[RuCl(dmso-*S*)$_3$(L)] has been characterized using single X-ray diffraction as well as spectroscopic techniques. This complex was then allowed to interact with DNA and its mode of binding with DNA and nuclease property in the presence of complex has been investigated.

2. Experimental

2.1. Materials and methods

Starting materials were purchased from Sigma–Aldrich and used without further purification. Infrared, UV–vis and luminescence spectra were recorded on VARIAN 3100 FTIR, JASCO V-630 spectrometer, and Perkin Elmer LS-45 spectrophotometer respectively. However, ^{1}H NMR and ^{13}C NMR spectra were recorded on JEOL AL 300 MHz spectrometer using TMS as internal reference. Elemental analysis and mass spectral measurements were carried out using a Carbo-Erba elemental analyzer 1108 and JEOL SX-102 mass spectrometer respectively. Cleavage experiments were performed

* Corresponding author. Tel.: +91 542 670 2449; fax: +91 542 236 8174.
E-mail address: lmishrabhu@yahoo.co.in (L. Mishra).

1010-6030/$ – see front matter © 2011 Elsevier B.V. All rights reserved.
doi:10.1016/j.jphotochem.2011.04.005

with the help of electrophoresis supported by Genei power supply with a potential range of 50–500 V, visualized and photographed by Vilber-INFINITY gel documentation system. The starting material *cis,fac*-[$RuCl_2$(dmso-*S*)$_3$(dmso-*O*)] was prepared from $RuCl_3 \cdot 3H_2O$ using reported procedure [11].

2.2. X-ray crystallographic studies

The crystal data were collected on Oxford diffraction XCALIBUR-S CCD area detector diffractometer using Mo Kα radiation (λ = 0.71073 Å) at 120 K and was solved by direct method and refined by full matrix least squares SHELXL-97 [12]. Drawings were carried out using MERCURY [13] and special computations were carried out with PLATON [14].

2.3. Binding studies of complex

2.3.1. Absorption titration

The concentration of DNA was determined by UV–vis absorbance using the molar absorption coefficient (6600 M^{-1} cm^{-1}) at 260 nm. The absorption ratio at 260 nm and 280 nm of CT DNA solutions was found as 1.9:1. It showed that DNA is sufficiently free from protein [15]. The absorption spectral titrations were performed using a fixed concentration of complex (100 μM) in Na-phosphate buffer (pH 7.2) containing DMSO (0.01%) while the concentrations of CT-DNA were varied within with 10–100 μM. From the absorption data, the intrinsic association constant with DNA was determined from a plot of [guest]/($\varepsilon_a - \varepsilon_f$) vs. [Host] using [16] Eq. (1)

$$\frac{[\text{guest}]}{(\varepsilon_a - \varepsilon_f)} = \frac{[\text{guest}]}{(\varepsilon_b - \varepsilon_f) + [K_b(\varepsilon_b - \varepsilon_f)]^{-1}} \quad (1)$$

where [guest] refers to the concentration of DNA (in base pair). The absorption coefficients ε_a, corresponds to A_{obsd}/[complex], ε_b and ε_f are the molar absorptivities of the fully bound and free form of the complex respectively. Plot of [DNA]/$\Delta\varepsilon$ vs. [DNA] (Scatchard plot) according to Eq. (1) gives the binding association constant K_b, are determined from the ratio of slope to the intercept.

2.3.2. Competitive binding with ethidium bromide

The relative binding of the complex to CT DNA was monitored by fluorescence spectral method using ethidium bromide (EB) bound to CT DNA solution in a Na phosphate buffer solution (pH 7.2). The solution of EB has been used as a spectral probe as it shows no apparent emission intensity in the buffer solution because of solvent quenching. However, enhanced emission intensity was observed when it intercalates to DNA [17]. The complex was allowed to interact with DNA-EB solution, the emission from the resulting solution was decreased. This decrease in emission-intensity could be considered in view of the replacement of EB (DNA bound) by the complex which consequently quenches the over-all emission-intensity. Competitive DNA binding studies of the complex with that of the ethidium bromide are carried out using recording of ethidium bromide fluorescence quenching after successive addition of 0–0.25 μM of complex to 10 μM DNA solutions containing 10 μM ethidium bromide in Na-phosphate buffer (pH 7.2). For this experiment, sample was excited at λ_{ex} 510 nm and emission spectra are recorded between 550 and 700 nm. Stern–Volmer quenching constant [18] was then calculated using the given equation

$$\frac{I_o}{I} = 1 + K_{sv}r \quad (2)$$

where I_o and I are the fluorescence intensities of the solution containing EB and DNA in the absence and presence of the complex respectively, K_{sv} is a linear Stern–Volmer quenching constant and r is the ratio of the total concentration of complex to that of DNA. The value of K_{sv} is given by the ratio of slope to intercept in a plot of I_o/I vs. [Complex]/[DNA].

2.3.3. Molecular docking study

MGL tools 1.5.4 with AutoGrid4 and AutoDock4 [19,20] were used to set up and perform blind docking calculations between the complex and DNA sequence. DNA sequence d(ACCGACGTCGGT)$_2$ obtained from the Protein Data Bank (PDB id: 423D) at a resolution of 1.60 Å was used for the docking studies. Due to unavailability of standard parameters for Ru (II) in autodock4 parameter file, Zn (II) parameters were used instead [21]. X-ray crystallographic coordinates were used for the complex for the docking study.

Receptor (DNA) and ligand (complex) files were prepared using AutoDock Tools. First of all the heteroatoms including water molecules were deleted and polar hydrogen atoms and Kollman charges were added to receptor molecule then rotatable bonds in ligands were assigned. All other bonds were allowed to rotate. The DNA was enclosed in a box with number of grid points in $x \times y \times z$ directions, $106 \times 100 \times 76$ and a grid spacing of 0.375 Å. Lamarckian genetic algorithms, as implemented in AutoDock, were employed to perform docking calculations. All other parameters were default settings. For each of the docking cases, the lowest energy docked conformation, according to the Autodock scoring function, was selected as the binding mode.

2.3.4. DNA cleavage

Cleavage experiments of supercoiled pBR322 DNA (300 ng) by complex (20–100 μM) in buffer (5 mM Tris–HCl/50 mM NaCl at pH 7.2), were carried out and the reaction was followed by agarose gel electrophoresis. The samples were incubated for 1 h at 37 °C. A loading buffer containing 25% bromophenol blue, 0.25% xylene cyanol, 30% glycerol was added and electrophoresis was carried out at 60 V for 1 h in Tris–HCl buffer using 1% agarose gel containing 1.0 μg/mL ethidium bromide. The reaction was also monitored upon addition of various radical inhibitors and/or activators such as dimethylsulphoxide (DMSO), sodium azide (NaN_3), superoxide dismutase (SOD), mercaptopropionic acid (MPA), glutathione (GSH), Hydrogen peroxide (H_2O_2), sodium ascorbate (Asc), groove binders; methyl green (MG) and 4′,6-diamidino-2-phenylindole (DAPI). The inhibition reactions were carried out by adding the reagent prior to the addition of the complex. The standard protocols were followed for these experiments. The samples were incubated for 45 min at 37 °C. The gel was visualized by photographing the fluorescence of intercalated ethidium bromide under a UV illuminator. The cleavage efficiency was measured by determining the ability of the complex to convert the supercoiled DNA (SC or Form I) to nicked circular form (NC or Form II) and linear form (LC or Form III).

2.4. Synthesis of (LH) 1-(2-hydroxyphenyl)-3-(4-chlorophenyl)propenone

The ligand 1-(2-hydroxyphenyl)-3-(4-chlorophenyl)propenone (LH) was synthesized using literature procedure [22] by the condensation of 2′-hydroxy acetophenone and ethanolic solution of 4-chlorobenzaldehyde in basic medium (50% NaOH). The ligand was further characterized by its spectral data and melting point (154–156 °C).

2.5. Synthesis and characterization of complex **1**

A hot methanolic solution (20 cm^3) of *cis,fac*-[$RuCl_2$(dmso-*S*)$_3$(dmso-*O*)] (0.484 g, 1 mmol) was added dropwise to a solution of LH (0.258 g, 1 mmol) dissolved in methanol (25 cm^3) containing equimolar NEt_3 while stirring. The reaction mixture was

then stirred further for 12 h at room temperature. A clear solution thus obtained was reduced to half of its volume under reduced pressure. The block shaped red crystals suitable for X-ray analysis were isolated from the solution in a refrigerator after 24 h. The crystals were filtered and washed with diethyl ether and then dried in vacuo. The crystals were partially soluble in water, hot ethanol and hot methanol but highly soluble in dichloromethane, acetonitrile, dimethylsulfoxide, chloroform, tetrahydrofuran and dimethylformamide. Yield: 0.300 g (45%). Elemantal analysis: For $C_{22}H_{32}Cl_2O_6S_3Ru$ Found: C, 39.85; H, 4.36 Cal.: C, 40.00; H, 4.88; ESI-MS: *m/z*: 627[M−H]$^+$, IR (KBr pellet, cm^{-1}): 3015(*m*) υ(C–H), 1620(*s*) υ(C=O), 1106(*s*) υ(S=O), 426(*m*) υ(Ru–S). ^{1}H NMR (300 MHz, $CDCl_3$, δ ppm): 3.09–3.55 (m, 18H; dmso), 2.14 (s, 3H; CH_3), 7.74, 6.89(d, 2H; HC=CH), 6.53–7.76(m, 8H; phenyl). ^{13}C NMR (75 MHz, $CDCl_3$): 188.501 (–C=O); 171.672 (PhC–O); 132.120, 133.422–(CH=CH); 115.307, 121.595, 122.469, 124.801, 125.642, 129.326, 136.735, 141.961 (Phenyl), 42.855, 44.132, 44.940, 46.003, 47.437 (DMSO). UV–vis (dmso, 10^{-4} M): λ_{max} (dmso)/nm (ε_{max} M^{-1} cm^{-1}) 262(5000), 336 (14190), 498^{sh} (2550). Crystallographic data: $C_{22}H_{32}Cl_2O_6RuS_3$, fw = 660.63, red block, monoclinic, C 2/c, a = 32.06(4) Å, b = 8.2776(17) Å, c = 25.34(4) Å, α = 90°, β = 126.69(2)°, γ = 90°, V = 5392(11) Å^3, Z = 8, D_c = 1.628 Mg/m^3, MoK\α radiation (λ = 0.71073 Å), 20557 reflections, 4736 with Full-matrix, least squares on F^2 used for refinement (R = 0.0326, wR2 = 0.0662, *GoF* = 0.893, hydrogens calculated).

2.6. Synthesis of **1**.gua

A solution of guanine (0.75 g, 0.5 mmol) in methanol (10 cm^3) containing few drops of aqueous HCl solution was added to a methanolic solution (10 cm^3) of complex 1 (0.330 g, 0.5 mmol) while stirring. It was refluxed for 3 h, the solution was then kept in a refrigerator. After 12 h, a yellow crystalline solid obtained, was filtered and washed with methanol. However, the solid adduct thus obtained was found unsuitable for its X-ray crystallographic study. It was found insoluble in water, dichloromethane, acetonitrile, chloroform, tetrahydrofuran, hot ethanol, hot methanol but it was found highly soluble in dimethylsulfoxide and dimethylformamide. Yield 0.200 g (56%) Anal. Calc. for $C_{24}H_{27}Cl_2N_5O_5S_2Ru$, Found (%): C, 41.7; H, 3.8; N, 9.8. Cal.: C, 41.1; H, 3.8; N, 9.9. FAB-MS: *m/z*: 700 [M]$^+$, 664[M−Cl]$^+$, 587[M−Cl-dmso]$^+$, 508 [M−Cl-2dmso]$^+$. IR (KBr pellet, cm^{-1}): 3327(m) υ(NH), 3037(m) υ(C–H), 1718(s), 1604(s) υ(C=O), 1668(s) (NH_2), 1099(s) υ(S=O), 420(m) υ(Ru–S). ^{1}H NMR (300 MHz DMSO, δ ppm): 3.09–3.55 (s, 12H; dmso), 12.430 (s, NH), 11.178 (s, NH), 6.76 (s, NH_2), 8.55(s, CH guanine), 8.23, 7.79(s, 2H; HC=CH), 6.98–8.085 (m, 8H; Ar). UV–vis (dmso, 10^{-4} M): λ_{max} (dmso)/nm (ε_{max} M^{-1} cm^{-1}) 418 (43104), 501^{sh} (4824).

3. Results and discussion

3.1. Structural characterization

The complex **1** was found air stable and non electrolyte in dimethylsulfoxide (10^{-3} M) solution. The complex displayed IR peaks at 1620, 1107 and 424 cm^{-1}, assigned to coordinated υ(C=O), υ(S=O) and υ(Ru–S) vibrations respectively. It showed that υ(C=O) vibration of free ligand (1639 cm^{-1}) shifted to lower wavenumber owing to its coordination with Ru(II) metal centre. Additionally υ(OH) vibration of the free ligand observed at 3047 cm^{-1} was not observed in the spectra of its complex. It showed that (OH) group of LH was deprotonated during coordination with the metal ion.

These assignments are further supported by ^{1}H NMR spectrum of the complex which showed peaks (δ ppm) at 3.09–3.55 (m, 18H; dmso), 7.74, 6.89 (d, 2H; HC=CH) and 6.53–7.76(m, 8H; phenyl). However, OH proton observed at δ 12.2 ppm in the spectrum of free LH disappered in the spectrum of the complex. The peaks displayed at (δ ppm.) 188.50, 171.67, 129.33 and 132.12, 115.30–141.96 in its ^{13}C NMR spectrum of complex were assigned to coordinated >C=O–, phenyl (–C–C–O–), CH=CH and phenyl carbon atoms respectively. The methyl carbon atoms of dimethylsulfoxide groups were displayed at δ 42.86–47.44 ppm.

Additionally, ESI-MS of the complex (S1) in methanol displayed an intense peak at m/z as 627 which corresponds to molecular ion [M−H]$^+$. Thus, ESI-MS together with NMR spectra recorded in solution suggested that complex is stable in solution.

The absorption spectrum of complex recorded in dichloromethane displayed band at λ_{max} 498 nm. This band is considered to arise from $d\pi(Ru^{II}) \rightarrow \pi^*(L)$ metal-to-ligand charge-transfer (MLCT) transitions [23]. However, bands observed at λ_{max} 262 nm, 337 nm are red shifted as compared to bands observed in the spectrum of the LH (λ_{max} 250 nm and 322 nm). These bands are attributed to intraligand and π–π^* type transitions respectively.

The crystals of the complex belong to rectangular shape monoclinic crystal system with space group C2/c and exhibit distorted-octahedral geometry around the low spin d^6 Ru(II) ion Fig. 1(a). It consists of a deprotonated chalcone (O, O) in bis-chelating mode (η^2), three *S*-coordinated dmso and one Cl. The chelating angle was found as 87.32°. A molecule of methanol was also detected in the molecular structure of the complex. The bond length data for Ru–O, Ru–S as well as Ru–Cl were comparable with Ru(II)-chloride–DMSO complexes. The two oxygen atoms of the chalcone are bonded to Ru(II) ion at 2.061(4) Å and 2.060(2) Å for Ru(1)–O(1) and Ru(1)–O(2) bonds respectively, slightly shorter than the corresponding values. However, Ru–S and Ru–Cl bond distances varied from 2.244(10) Å to 2.274(4) Å and 2.424(3) Å respectively and found longer than the reported values [23].

A PLATON analysis showed the formation of one conventional hydrogen bond and twelve non-conventional hydrogen bonds (S2). The non conventional bonds are formed through a DMSO molecule as H-donor (CH_3) while its O atom together with a Cl atom acted as H-acceptors. The crystal packing of the complex displayed independent inter-chain (O–H=O) formation. The inter-chain hydrogen bond was formed between the O–H group of the coordinated methanol molecule and uncoordinated oxygen of DMSO at a distance of 2.768(7) Å with O–H–O angle of 173° as depicted in Fig. 1(b). Molecular structure of complex also displayed the presence of extensive intra- and intermolecular C–H–Cl interaction. The packing diagram of complex along crystallographic axis *c* forms butter fly structure. It clearly shows formation of a double helical arrangement supported by co-crystallized methanol molecules. The Cl atom play important role in the formation of this network through CH···Cl interaction. The packing diagram of complex along crystallographic axis *c* forms supramolecular network (butter fly structure) as depicted in Fig. 2. It clearly shows the formation of a double helical arrangement supported by co-crystallized methanol molecules. The Cl atom play important role in the formation of this network through CH···Cl interaction. The Kitaigorodskii packing index [24] of 70.4% with no grid points indicated compact packing in its crystal lattice.

To understand the binding mode of the complex with DNA base on preliminary level, a complex of the composition Ru(L)(dmso)$_2$guaCl (**1**.gua) was isolated and characterized. Its molecular composition was further supported by its mass at *m/z* 700 assigned to [M]$^+$ (S3). Thus, the composition of the complex showed that one DMSO coordinated in complex **1** is substituted by one guanine molecule and the resulting complex **1**.gua was found air stable and soluble in dimethyl sulphoxide and dimethyl-

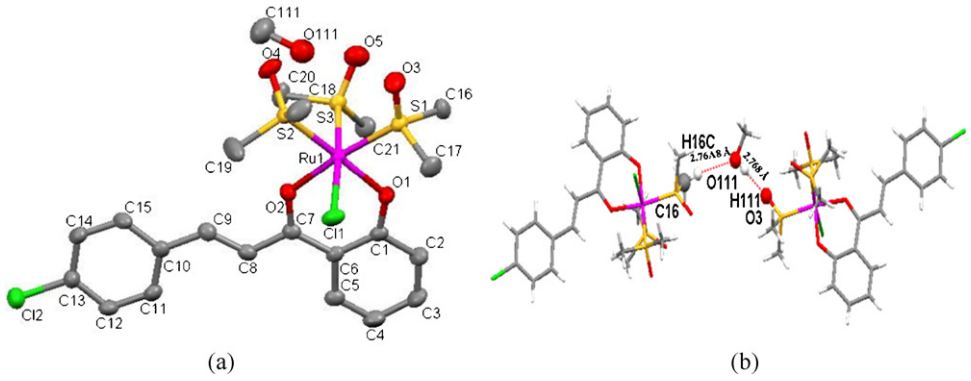

Fig. 1. (a) Molecular structure of complex with 50% probability ellipsoid (H atoms omitted for clarity). (Selected bond length and bond angles: Ru(1)–O(2) = 2.060 Å, Ru(1)–O(1) = 2.061 Å, Ru(1)–S(1) = 2.244 Å, Ru(1)–S(3) = 2.271 Å, Ru(1)–S(2) = 2.274 Å, Ru(1)–Cl(1) = 2.424 Å, Cl(2)–C(13) = 1.734 Å, S(1)–O(3) = 1.487 Å, S(1)–C(16) = 1.757 Å, O(1)–C(1) = 1.305 Å, O(2)–C(7) = 1.282 Å, O(2)–Ru(1)–O(1) = 87.32°, O(2)–Ru(1)–S(1) = 172.85°, S(1)–Ru(1)–S(3) = 92.91°, O(1)–Ru(1)–Cl(1) = 87.71°, S(3)–Ru(1)–Cl(1) = 173.83°, O(3)–S(1)–C(16) = 106.56°, C(16)–S(1)–C(17) = 98.2°, C(16)–S(1)–Ru(1) = 110.38°, O(4)–S(2)–Ru(1) = 121.11°, O(1)–C(1)–C(6) = 126.1°) and (b) Two molecules of complex linked to a methanol (CH_3OH) through C–H···O interaction.

formamide. Its IR spectrum displayed peaks at 1668, 1604, 1099, 1718 and 3327 cm^{-1} which were assigned to coordinated $\delta(NH_2)$, υ(C=O) (due to chalcone), υ(S=O) υ(C=O) (due to guanine) and $\upsilon(NH_2)$ vibrations. The δ (NH_2), υ(C=O) and $\upsilon(NH_2)$ vibrations of free guanine were shifted to lower energy in the spectrum of **1**.gua. It could be considered owing to its coordination with the metal ion in view of earlier report [25].

In general, coordination of nucleobase, nucleoside and nucleotide to ruthenium ion displays H8 proton of the corresponding nucleobases to upfield and considerably more broadened owing to its closer proximity to the metal centre [26]. In the ^{1}H NMR spectrum of **1**.gua, H8 proton appeared at δ = 8.55 ppm which is upfield as compared to H8 proton of free guanine observed at δ = 8.94 ppm. Thus, it is considered that one guanine molecule is coordinated to Ru(II) centre via its N7 atom.

The UV–vis spectrum of **1**.gua recorded in DMSO (10^{-4} M) showed intraligand π–π^* transitions at λ_{max} 418 nm. This band was red shifted as compared to intraligand transition observed in the spectrum of complex **1** (λ_{max} 337 nm). The other band observed at λ_{max} 502 nm is assigned to MLCT transition.

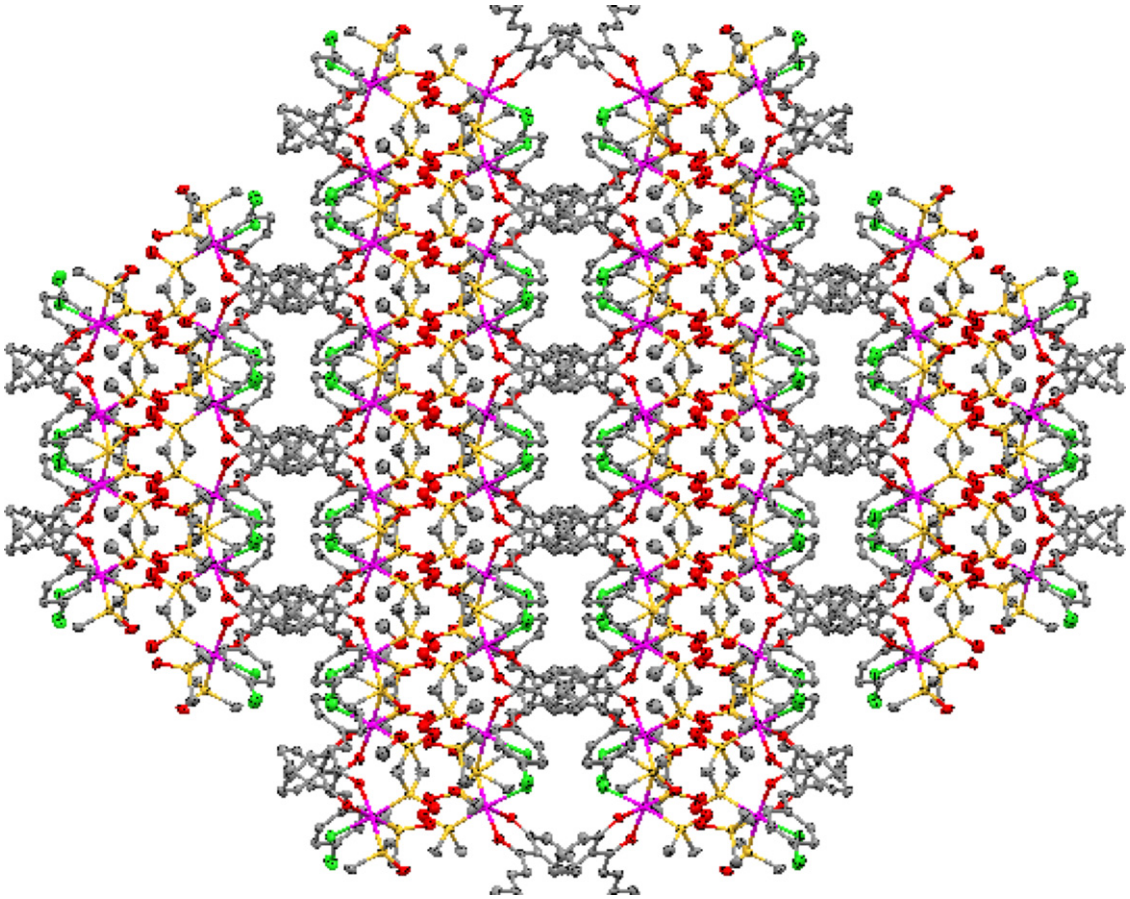

Fig. 2. The packing diagram of complex (butter fly structure) along crystallographic axis *c*.

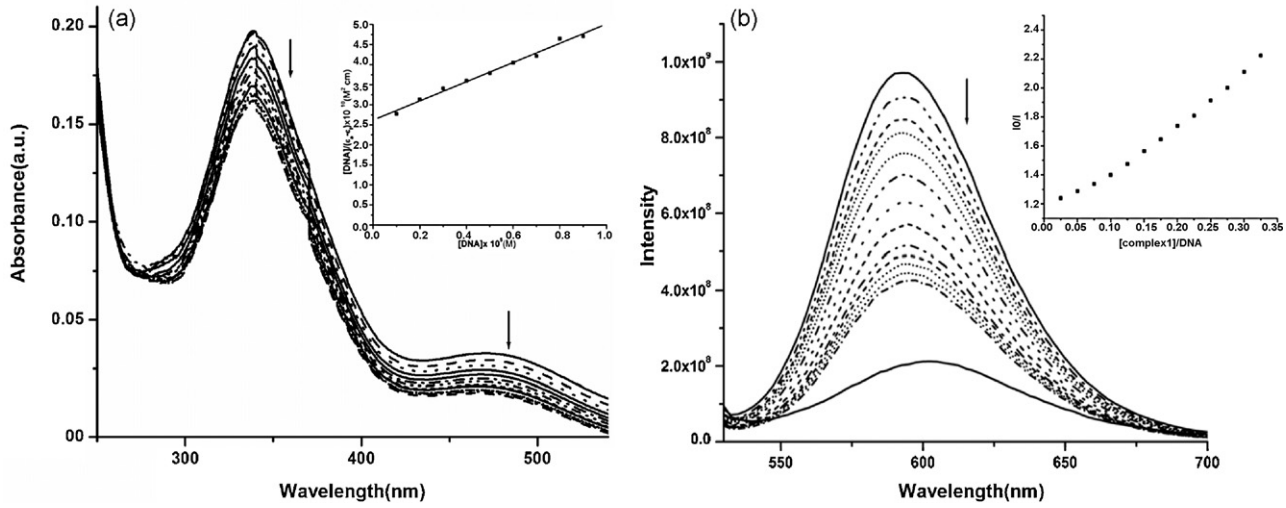

Fig. 3. (a) Absorption spectra of [Complex] = 100 μM in the absence and presence of increasing concentration of DNA = 10–100 μM. Arrow shows the absorbance changes upon increasing DNA concentrations (inset: plot of $[DNA]/(\varepsilon_a - \varepsilon_f)$ vs. [DNA].) and (b) fluorescence quenching pattern of ethidium bromide bound to DNA by complex. [EB] = 10 μM, [DNA] = 10 μM, [Complex] = 0–0.67 μM. Arrow shows the intensity changes upon increasing complex concentrations. (Inset: Plot of I_o/I vs. [complex]/[DNA]).

3.2. CT-DNA interaction with complex using UV–Vis spectroscopy

Electronic absorption spectroscopy is an effective method to examine the binding mode of DNA with metal complexes [27]. It has been reported earlier [27] that intercalation of a metal complex with DNA involves π^* orbital of the intercalated ligand which may couple with the π orbital of the DNA base pairs, concomitantly lowers the π–π^* transition energy hence displays a bathochromic shift in the transition. On the other hand, the coupling of a π orbital with partially filled electrons decreases the transition probabilities hence results hypochromic shift [28]. Thus, such observation prompted us to investigate the binding of newly prepared complex with DNA using spectroscopic titrations of a solution of the complex with CT-DNA. On increasing the CT-DNA concentration, a hypochromic shifts in both chalcone centered band and MLCT band were observed. The complex can bind with double-stranded DNA in various binding modes on the basis of its structure. However, hypochromic effect could be attributed to the stacking interaction between the aromatic rings of the ligand framework and DNA base pairs as well. The hypochromism and bathochromic shifts may commonly vary in consistence with the strength of intercalative interaction of the complex with DNA helix as well as overall conformation of the DNA. The intrinsic binding constant (K_b) was calculated by plotting the changes in the absorbance of the complex upon incremental addition of increasing concentration of DNA as shown in Fig. 3(a). The significant magnitude of binding constant ($K_b = 3.8 \times 10^7$) obtained from the ratio of slope to the intercept from the plots of $[DNA]/(\varepsilon_a - \varepsilon_f)$ vs. [DNA] showed many folds stronger binding with DNA as compared to the earlier reported values for ruthenium–porphyrin complex [29] as well as ruthenium–ammine complexes [30,31].

3.3. Competitive binding of complex with ethidium bromide using flouresence spectroscopy

The ability of a complex to change the fluorescence intensity of ethidium bromide (EB) in its EB-DNA adduct has been reported as a standard intercalating agent of DNA and it is a reliable tool to measure the affinity of the complex for DNA, irrespective of the binding modes. Therefore, a solution of EB has been used as a spectral probe since it does not emit in the buffer solution due to probable quenching of its emission by the solvent [32]. However, intense emission is observed when EB strongly intercalates with the adjacent DNA base pairs. But a decrease in emission intensity results from the displacement of EB by a quencher molecule. The extent of emission quenching could be used to determine the extent of binding between the metal complex with DNA. The emission spectra of EB-DNA system in the absence and presence of complex are displayed in Fig. 3(b). The quenching plot between I_o/I vs. [Complex]/[DNA] is in good agreement with the linear Stern–Volmer equation and Stern–Volmer quenching constant (K_{sv}) is calculated as 3.2.

3.4. Molecular docking of the complex with DNA sequence d(ACCGACGTCGGT)$_2$

After satisfactory spectroscopic measurement of DNA binding study of the complex, molecular docking study was performed to understand the preferred orientation of sterically acceptable complex using chalcone ligand with the DNA sequence. According to this docking experiment, complex reasonably bind with DNA sequence d(ACCGACGTCGGT)$_2$. The minimum energy docked structure obtained (Fig. 4) suggested the best possible conformation of the ligand interaction mainly through phenyl ring inside the DNA major groove. It has been observed that the complex is stabilized by electrostatic hydrogen bonding with DNA bases, particularly involving N^6 of adenine from chain A and N^7 of guanine from the chain B, in addition to van der Waal's and stacking π–π bond interactions between electron deficient chalcone ring system and purine–pyrimidine bases. Dimethyl sulfoxide (dmso) coordinated to Ru(II) ion, participates in hydrogen bonding whereas the side chains attached to Ru(II) complex enabled the molecules to stay in the groove with the help of van der Waals forces. The binding energy values presented in Table 1a suggested that van der Waal interactions are dominant over electrostatic interactions. The hydrogen bonding interactions involving the energy-minimized Docked poses of d(ACCGACGTCGGT)$_2$ with complex and is shown in Table 1b.

Thus, molecular docking study together with spectroscopic studies indicated that complex **1** interacts with the DNA through both covalent and non-covalent interactions which perhaps owe to its stronger bonding with DNA.

Table 1a
Molecular docking parameters of complex **1**.

Binding energy Kcal/mole	Inter-mol energy Kcal/mole	Vdw_hb_desolv energy Kcal/mole	Electrostatic energy Kcal/mole	Total internal energy Kcal/mole	Torsional energy Kcal/mole
−8.24	−10.62	−10.42	−0.2	−1.23	2.39

Table 1b
Hydrogen bonding interactions involving the energy-minimized docked poses of $d(ACCGACGTCGGT)_2$ with complex **1**.

Acceptor group (Y-H)	Donor group Z	Distance (Å)
H(N6)(A5)(DNA-chain A)	O5(complex)	2.096
H(N7)(G19)(DNA-chain B)	O4(complex)	1.963

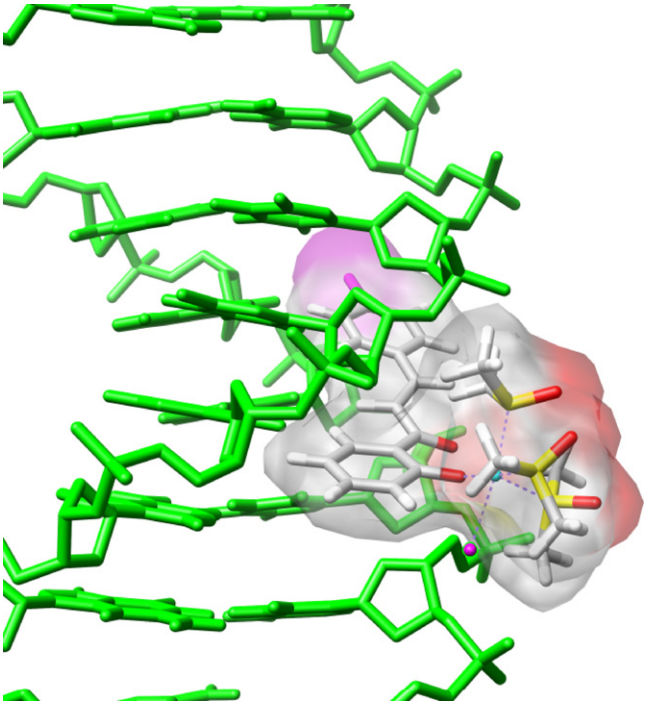

Fig. 4. Molecular docking of the complex **1** with DNA.

3.5. DNA cleavage activity

3.5.1. DNA cleavage in presence of complex

After exploring strong binding of the complex with CT DNA both experimentally and theoretically, the nuclease activity of the complex was analyzed by monitoring the unwinding of supercoiled pBR322 plasmid DNA (Form I) to nicked DNA (Form II) or Linear circular (Form III). The amounts of strand scission were assessed by agarose gel electrophoresis. A concentration-dependent DNA cleavage experiment was performed, by mixing pBR322 DNA with different concentrations (20–100 μM in acetonitrile) of ruthenium complex in buffer (5 mM Tris–HCl/50 mM NaCl at pH 7.2) and the mixture was then incubated at 310 K for 30 min. The cleavage patterns as a consequence of increasing concentration of the complex showed conversion of supercoiled (Form I) into the nicked circular form (Form II) without conversion to linear circular form (Form III) and are depicted in Fig. 5(a). Thus, it indicated that complex is involved in single strand DNA cleavage. The complex converts more than 90% of SC form into NC form at a concentration of 100 μM.

The nuclease efficiency of complexes is usually dependent on activators. Therefore, to understand the cleavage mechanism, a lower concentration (40 μM) of the complex was allowed to stay in the presence of some activators like H_2O_2, 3-mercaptopropionic acid (MPA) and glutathione (GSH). The degrees of binding of complex to DNA in presence of H_2O_2, ASC, MPA, GSH were found as 74%, 43%, 40%, and 30%, respectively. As displayed in Fig. 5(b), the nuclease activity of complex was significantly enhanced in the presence of activators and their activating efficacy follows the order of H_2O_2 > ASC > MPA > GSH.

3.5.2. DNA cleavage in presence of minor and major groove binding agents

The potential interacting site of the complex with supercoiled plasmid pBR322 DNA was performed by recognition elements, minor groove binding agent 4′,6-diamidino-2-phenylindole (DAPI) and major groove binding agent methyl green (MG) [33]. The supercoiled DNA was treated separately with DAPI and MG prior to the addition of the complex. The degree of binding of the complex with pBR322 DNA in presence of DAPI and MG was found as 38% and 66% respectively. Thus, present complex binds DNA through its major groove, Fig. 6(a) which supports the result obtained from molecular docking study.

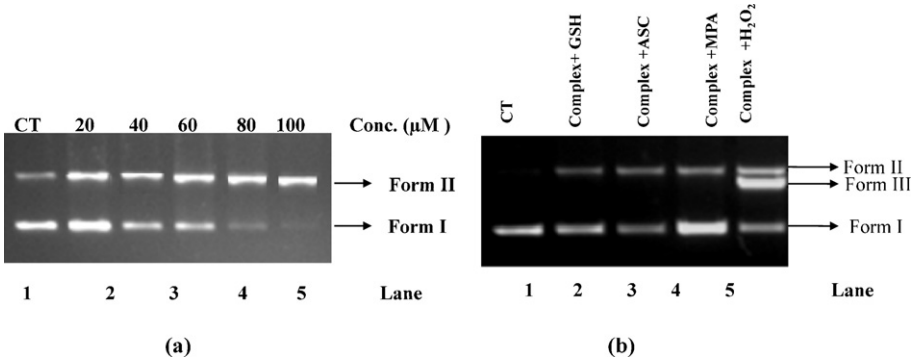

Fig. 5. (a) Agarose gel electrophoresis showing cleavage patterns of the for pBR322 plasmid DNA (300 ng) by the complex. Lane 1, DNA; Lane 2, 20 μM complex + DNA; Lane 3, 40 μM complex + DNA; Lane 4, 60 μM complex + DNA; Lane 5, 80 μM complex + DNA; Lane 6, 100 μM complex + DNA and (b) agarose gel electrophoresis pattern for the cleavage pattern of pBR322 plasmid DNA (300 ng) by lower concentration (40 μM) of the complex in presence of different activating agents. Lane 1, DNA control; Lane 2, DNA + complex + GSH (0.4 mM); Lane 3, DNA + complex + Asc (0.4 mM); Lane 4, DNA + complex + MPA (0.4 mM); Lane 5, DNA + complex + H_2O_2 (0.4 mM).

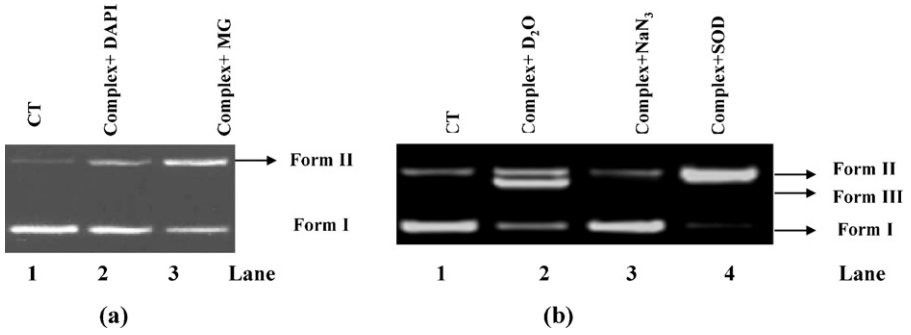

Fig. 6. (a) Agarose gel electrophoresis pattern for the cleavage pattern of pBR322 plasmid DNA (300 ng) by the complex (40 μM). Lane 1, DNA control; Lane 2, DNA + complex + DAPI (8 μM); Lane 3, DNA + complex + methyl green (2.5 μL of a 0.01 mg/mL solution) and (b) agarose gel electrophoresis pattern showing cleavage of pBR322 plasmid DNA (300 ng) by the complex (80 μM). Lane 1, DNA control; lane 2, DNA + complex + D_2O (70%); Lane 3, DNA + complex + NaN_3 (0.4 mM); Lane 8, DNA + complex + superoxide dismutase (15 Units), respectively.

The experiments were further carried out in presence of several reactive oxygen trappers in view of the report that interaction between a metal complex and dioxygen or redox reagents is believed to be a major cause of DNA damage. Thus, to investigate this mechanistic pathway of the DNA cleavage, the complex was allowed to interact with DNA separately with tert-butyl alcohol and DMSO as a hydroxyl radical scavenger under identical conditions. But cleavage was not significant as compared to DNA cleavage without them. Therefore, it was considered that diffusible ($^{\bullet}OH$) hydroxyl radicals are not responsible for DNA cleavage (S4). However, with other oxygen trappers like sodium azide as singlet oxygen scavenger, the cleavage was significantly exhibited, revealing the involvement of $^1O_2$ in the DNA cleavage. The involvement of $^1O_2$ was further supported by the significant enhancement of the cleavage activity in D_2O, where lifetime of $^1O_2$ is notably longer than that in water [34]. In D_2O, a linear form also appears that indicated increase in the cleavage. However, presence of superoxide dismutase (SOD), a facile superoxide anion radical ($O_2^{\bullet-}$) quencher, cleavage was observed similar to that observed in presence of complex only. It revealed that superoxide anion is not active specie in the cleavage of pBR322 DNA as depicted in Fig. 6(b). Hence, the cleavage pattern thus observed supported the oxidative cleavage pathway.

4. Conclusion

The newly synthesized complex, *cis,fac*-[RuCl(dmso-*S*)$_3$(L)] **1** interacts strongly with DNA using both covalent and non-covalent interactions as monitored by UV–vis and emission titrations followed by molecular docking and gel electrophoresis under physiological conditions. To understand the coordinate binding of a nucleo base with the complex **1**, its adduct with guanine was prepared and characterized. The complex **1** cleaves DNA without the use of any exogenous agents. But in the presence of minor and major groove binding agents, complex showed preferred binding with DNA via its major groove. These studies suggested that cleavage of DNA most likely follows the oxidative pathway.

Supporting information available

CCDC reference number 750138 contains the crystallographic data for complex. These data can be obtained free of charge via http://www.ccdc.cam.ac.uk/conts/retrieving.html, or from the Cambridge Crystallographic Data Centre, 12 Union Road, Cambridge CB2 1EZ, UK, fax (+44) 1223-336-033, or e-mail: deposit@ccdc.cam.ac.uk. ESI-MS of complex **1**, selected parameters for weak interactions in complex, FAB mass of **1**.gua, and nuclease activity in presence of trappers.

Acknowledgements

Authors are grateful to authorities of DBT and UGC, New Delhi India for their financial supports.

Appendix A. Supplementary data

Supplementary data associated with this article can be found, in the online version, at doi:10.1016/j.jphotochem.2011.04.005.

References

[1] K.E. Erkkila, D.T. Odom, J.K. Barton, Chem. Rev. 99 (1999) 2777–2796.
[2] B. Lippert, Coord. Chem. Rev. 200 (2000) 487–516.
[3] A. Levina, A. Mitra, P.A. Lay, Metallomics 1 (2009) 458–470.
[4] M.J. Clarke, Coord. Chem. Rev. 236 (2003) 207–231 (and references there in).
[5] J.K. Barton, E. Lolis, J. Am. Chem. Soc. 107 (1985) 708–709.
[6] N. Dixit, L. Mishra, Inorganic Biochemistry Research Progress, Nova Science Publishers, New York, United States, 2008, pp. 105–159.
[7] H. Chen, J.A. Parkinson, S. Parsons, R.A. Coxall, R.O. Gould, P.J. Sadler, J. Am. Chem. Soc. 124 (12) (2002) 3064–3082.
[8] X. Wu, P. Wilairat, M.L. Go, Bioorg. Med. Chem. Lett. 12 (2002) 2299–2302.
[9] Z. Nowakowska, Eur. J. Med. Chem. 42 (2007) 125–137.
[10] B.E. Evans, K.E. Rittle, M.G. Bock, R.M. Dipardo, R.M. Freidinger, W.L. Whitter, G.F. Lundell, D.F. Veber, P.S. Anderson, R.S.L. Chang, V.J. Lotti, D.J. Cerino, T.B. Chen, P.J. Kling, K.A. Kunkel, J.P. Springer, J. Hirshfield, J. Med. Chem. 31 (1988) 2235–2246.
[11] E. Alessio, G. Mestroni, G. Nardin, W.M. Attia, M. Calligaris, G. Sava, S. Zorzet, Inorg. Chem. 27 (1988) 4099–4106.
[12] G.M. Sheldrick, Acta Crystallogr. A 64 (2008) 112–122.
[13] I.J. Bruno, J.C. Cole, P.R. Edgington, M. Kessler, C.F. Macrae, P. McCabe, J. Pearson, R. Taylor, MERCURY, Acta Cryst. B 58 (2002) 389–397.
[14] A.L. Spek, PLATON package, Acta Crystallogr. D 65 (2009) 148–155.
[15] J. Marmur, J. Mol. Biol. 3 (1961) 208–218.
[16] A. Wolfe, G.H. Shimer, T. Meehan, Biochemistry 26 (1987) 6392–6396.
[17] N. Dixit, R.K. Koiri, B.K. Maurya, S.K. Trigun, C. Höbartner, L. Mishra, J. Inorg. Biochem. 105 (2011) 256–267.
[18] J.R. Lakowicz, Principles of Fluorescence Spectroscopy, second ed., Plenum Press, New York, 1999, p. 698.
[19] G.M. Morris, R. Huey, W. Lindstrom, M.F. Sanner, R.K. Belew, D.S. Goodsell, A.J. Olson, J. Comput. Chem. 30 (2009) 2785–2791.
[20] G.M. Morris, R. Huey, A.J. Olson, Using AutoDock for ligand-receptor docking, Curr. Protoc. Bioinf. 8 (2008), unit 14.1–8.14.
[21] A. Loosli, U.E. Rusbandi, J. Gradinaru, K. Bernauer, C.W. Schlaepfer, M. Meyer, S. Mazurek, M. Novic, R. Thomas Ward, Inorg. Chem. 45 (2) (2006) 660–668.
[22] Y.R. Prasad, A.L. Rao, R. Rambabu, E-J. Chem. 5 (3) (2008) 461–466.
[23] R. Prajapati, S.K. Dubey, R. Gaur, R.K. Koiri, B.K. Maurya, S.K. Trigun, L. Mishra, Polyhedron 29 (2010) 1055–1061.
[24] A.I. Kitaigorodskii, Molecular Crystals and Molecules, Academic Press, New York, 1973.
[25] A. Abo-riziq, B.O. Crews, I. Compagnon, Jos. Oomens, G. Meijer, G.V. Helden, M. Kabela, P. Hobza, M.S. DeVries, J. Phys. Chem. A 111 (2007) 7529–7536.

[26] V.M. Rodriguez-Bailey, K.J. LaChance-Galang, P.E. Doan, M.J. Clarke, Inorg. Chem. 36 (1997) 1873–1883.
[27] A.M. Pyle, J.P. Rehmann, R. Meshoyrer, C.V. Kumar, N.J. Turro, J.K. Barton, J. Am. Chem. Soc. 111 (1989) 3053–3063.
[28] H. Chao, W.J. Mei, Q.W. Huang, L.N. Ji, J. Inorg. Biochem. 92 (2002) 165–170.
[29] S. Rani-Beeram, K. Meyer, A. McCrate, Y. Hong, M. Nielsen, S. Swavey, Inorg. Chem. 47 (2008) 11278–11283.
[30] M.J. Clarke, B. Jansen, K.A. Marx, R. Kruger, Inorg. Chim. Acta 124 (1986) 13–28.
[31] P.U. Maheswari, M. Palaniandavar, J. Inorg. Biochem. 98 (2004) 219–230.
[32] M.J. Waring, J. Mol. Biol. 13 (1965) 269–282.
[33] G.-J. Chen, X. Qiao, J.-L. Tian, J.-Y. Xu, W. Gu, X. Liu, S.-P. Yan, Dalton Trans. 39 (2010) 10637–10643.
[34] D. Lahiri, T. Bhowmick, B. Pathak, O. Shameema, A.K. Patra, S. Ramakumar, A.R. Chakravarty, Inorg. Chem. 48 (2009) 339–349.